JHEP

Published for SISSA by Springer

Received: November 17, 2023
Accepted: December 7, 2023
Published: December 20, 2023

JHEP12(2023)147

$\mathcal{O}\left(m\alpha^2(Z\alpha)^6\right)$ contribution to Lamb shift from radiative corrections to the Wichmann-Kroll potential

Petr A. Krachkov and Roman N. Lee

Budker Institute of Nuclear Physics,
Lavrentiev ave. 11, Novosibirsk 630090, Russia

E-mail: p.a.krachkov@inp.nsk.su, r.n.lee@inp.nsk.su

Abstract: We derive an analytical expression for the contribution of the order $m\alpha^2(Z\alpha)^6$ to the hydrogen Lamb shift which comes from the diagrams for radiative corrections to the Wichmann-Kroll potential. We use modern methods of multiloop calculations, based on IBP reduction, DRA method and differential equations.

Keywords: Higher Order Electroweak Calculations, Precision QED

ArXiv ePrint: 2311.05860

https://doi.org/10.1007/JHEP12(2023)147

Contents

JHEP12(2023)147

1 Introduction

Recent advances in spectroscopy of ordinary hydrogen [1, 2] and deuterium [3] and in their muonic analogs [4, 5] as well as in the electron-proton scattering [6] provide new opportunities to perform subtle tests of the bound-state quantum electrodynamics (QED).

The hydrogen atom is a system in which the role of the relativistic, radiative, and recoil effects can be investigated with high precision, both experimentally and theoretically. The corresponding corrections to energy levels are small compared to the leading term. However, with the present accuracy achieved in measuring the frequency of specific hydrogenic transitions, those contributions are large compared with the experimental uncertainty.

One of the most important bound-state QED effects is the Lamb shift. It is responsible for the $2s_{1/2}$–$2p_{1/2}$ energy splitting, which in the Dirac equation approximation would be zero. The calculations of various contributions to the Lamb shift have a long history starting from refs. [7–10], see also [11–14] and references therein. For the s-states all corrections have been calculated up to the order $m\alpha^2(Z\alpha)^6 \ln\left(1/(Z\alpha)^2\right)$. The $m\alpha^2(Z\alpha)^6$ contribution has not yet been calculated, although this correction may be important already in the next series of spectroscopic measurements.

In the present paper we calculate one of the previously unknown corrections[1] to the Lamb shift of order $m\alpha^2(Z\alpha)^6$, which is connected with the radiative corrections to the Wichmann-Kroll (WK) potential.

We use modern multiloop methods, based on the integration by parts (IBP) reduction [16, 17], differential equations approach [18, 19], and dimensional recurrence and analyticity (DRA) method [20, 21]. Recently, we applied similar approach to the calculation of certain two-loop corrections to Lamb shift and hyperfine splitting in hydrogen, ref. [22]. In contrast to ref. [22], in the present work we are able to obtain the analytic result in terms of conventional polylogarithmic constants only. The present calculation provides yet another example of the effectiveness of multiloop methods for obtaining analytic results in atomic physics.

[1] A heuristic estimate of the magnitude of this contribution was given in ref. [15].

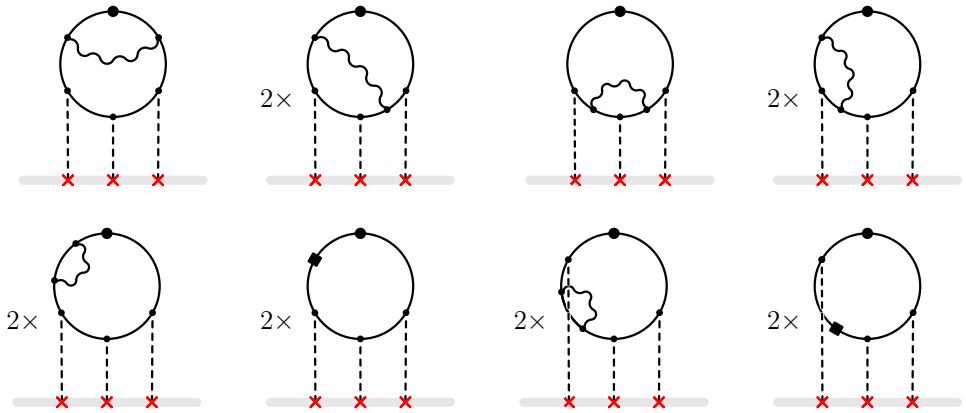

(a) Diagrams with one electron loop. Black squares correspond to the mass counter term $i\delta m$.

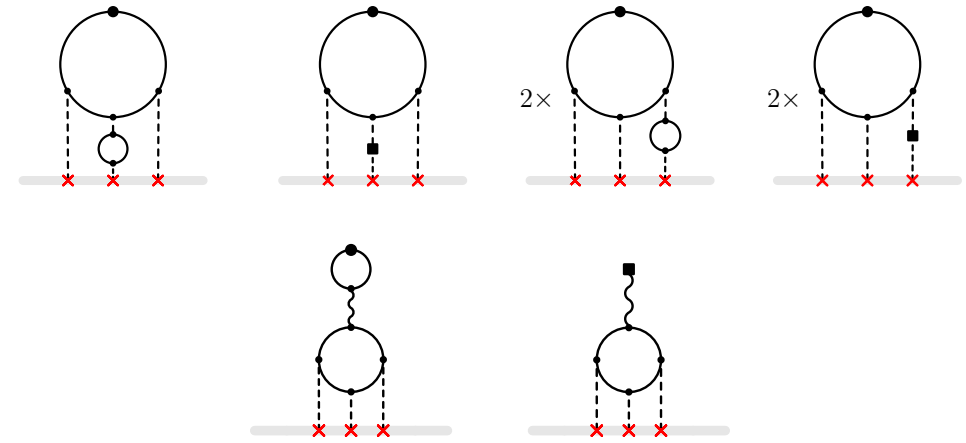

(b) Diagrams with two electron loops. Black squares correspond to the vertex $-i\delta Z_A(q^2 g_{\mu\nu} - q_\mu q_\nu)$.

Figure 1. Feynman diagrams corresponding to the radiative corrections to the Wichmann-Kroll charge density $\delta\tilde{\rho}(q)$. Big black dot on the top of the diagrams corresponds to the insertion of $-ie\gamma^0$ vertex.

2 Energy shift due to radiative correction to WK potential

Feynman diagrams for the radiative correction $\delta\tilde{\rho}(q)$ to the Wichmann-Kroll charge density are depicted in figure 1. On the same figure we also show the diagrams with one-loop conterterms. The black squares on solid lines correspond to the mass counter terms $i\delta m = im\frac{(4\pi\alpha)m^{-2\epsilon}(3-2\epsilon)\Gamma(\epsilon)}{(4\pi)^{2-\epsilon}(1-2\epsilon)}$, while the black squares on dashed lines correspond to $-i\delta Z_A(q^2 g_{\mu\nu} - q_\mu q_\nu) = i\frac{(16\pi\alpha)m^{-2\epsilon}\Gamma(\epsilon)}{3(4\pi)^{2-\epsilon}}(q^2 g_{\mu\nu} - q_\mu q_\nu)$. In principle, we should also account for the diagrams with one-loop fermion field renormalization and vertex counterterms, but their contributions cancel due to the Ward identity.

The corresponding correction to the potential $\delta\widetilde{V}(q) = \delta\tilde{\rho}(q)\cdot(e/q^2)$ contributes to energy shifts. The characteristic atomic momenta q are small compared to the electron

JHEP12(2023)147

mass. Therefore, we need the small-q asymptotics of $\tilde{\rho}(q)$. This asymptotics can be analyzed using the expansion by regions approach. There are two regions which are relevant to this asymptotics. The hard region corresponds to all loop momenta $\sim m$. In this region we expand the integrand of $\delta\tilde{\rho}(q)$ in Taylor series in q. The zeroth term corresponds to the sum of diagrams in figure 1 at $q = 0$. It is easy to see that, due to the identity

$$\sum_{k=1}^{N} \mathrm{Tr}\left[\gamma^{\mu_1}(\hat{p}-\hat{l}_1-m)^{-1}\dots\gamma^{\mu_k}(\hat{p}-\hat{l}_k-m)^{-1}\gamma^{\alpha}(\hat{p}-\hat{l}_k-m)^{-1}\dots\gamma^{\mu_N}(\hat{p}-\hat{l}_N-m)^{-1}\right]$$
$$= -\frac{\partial}{\partial p_\alpha}\mathrm{Tr}\left[\gamma^{\mu_1}(\hat{p}-\hat{l}_1-m)^{-1}\dots\gamma^{\mu_N}(\hat{p}-\hat{l}_N-m)^{-1}\right], \tag{2.1}$$

this sum can be written as the integral of total derivative which is zero in dimensional regularization. The sum in the left-hand side of the above identity corresponds to all possible insertions of the vertex γ^α in the fermion loop.

The contribution to $\delta\tilde{\rho}(q)$ linear in $\boldsymbol{q}$ is zero due to rotation symmetry. Therefore, the expansion in the hard region starts from q^2 term,

$$\delta\tilde{\rho}(q) \approx (\delta\widetilde{V}(0)/e)\cdot q^2. \tag{2.2}$$

Note that the sum of the two diagrams on the last row of figure 1b is suppressed by an additional factor q^2, therefore, they can be neglected within our present accuracy.

There is also a soft region, corresponding to all momentum transfers to the nucleus $q_1, q_2, q_3 = q - q_1 - q_2$ being small. Due to the gauge invariance of the light-by-light block it is easy to see that the corresponding contribution starts from $q^{4-4\epsilon}$, which is also too small for our present accuracy.

Eq. (2.2) shows that the potential $V(\boldsymbol{r}) = e\int e^{i\boldsymbol{q}\boldsymbol{r}}\delta\tilde{\rho}/q^2 d\boldsymbol{q}/(2\pi)^3$ is proportional to the delta function and the Lamb shift contribution can be written as:

$$\delta E = |\psi_{n\ell}(0)|^2\delta\widetilde{V}(0) = m\frac{\alpha^2(Z\alpha)^6}{\pi^2 n^3}B\delta_{\ell,0}\,, \tag{2.3}$$

where B is a numerical coefficient to be calculated, m is the electron mass, n and ℓ are the principal and angular quantum numbers, respectively.

3 Calculation and result

The small-q expansion of the diagrams in figure 1 can be expressed in terms of the integrals of the family

$$j(n_1,\cdots,n_{14}) = \int\frac{dq_1 dq_2 dl_1 dl_2}{\pi^{2d}}\prod_{k=1}^{12}D_k^{-n_k}\times\prod_{s=13}^{14}\frac{\delta^{(n_s-1)}(D_s)}{(n_s-1)!}\,, \tag{3.1}$$

where

$$\begin{aligned}
&D_1 = 1-l_1^2\,, && D_2 = 1-l_2^2\,, && D_3 = 1-(l_2-q_2)^2\,, &&\\
&D_4 = 1-(l_2+q_1)^2\,, && D_5 = 1-(l_1+q_1)^2\,, && D_6 = -(l_1-l_2)^2\,, &&\\
&D_7 = -q_1^2\,, && D_8 = -q_2^2\,, && D_9 = -(q_1+q_2)^2\,, && D_{10} = (l_1 n)\,,\\
&D_{11} = (l_2 n)\,, && D_{12} = (l_1-q_2)^2\,, && D_{13} = (q_1 n)\,, && D_{14} = (q_2 n)\,.
\end{aligned} \tag{3.2}$$

JHEP12(2023)147

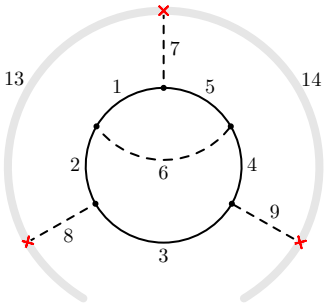

Figure 2. Topology corresponding to the integral family in eq. (3.1). Numbers correspond to the subscript k of the denominator D_k in eq. (3.2).

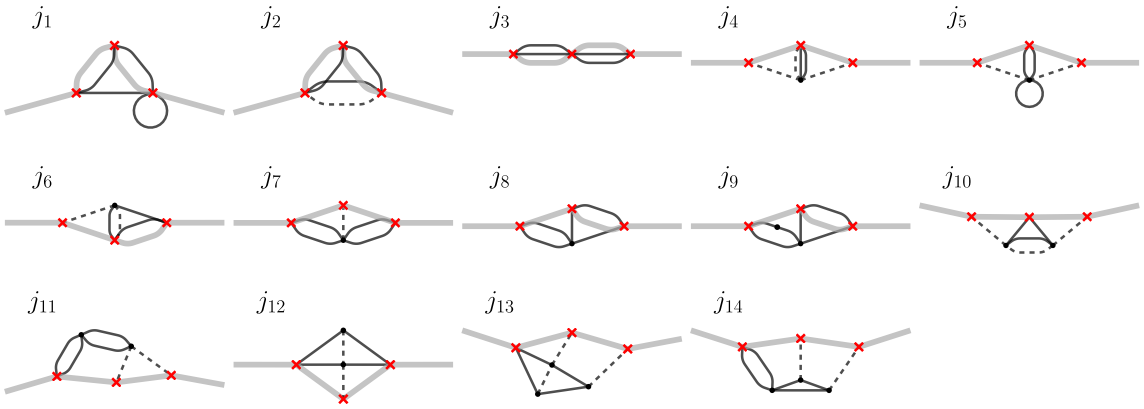

Figure 3. Master integrals.

Here $n = (1, \mathbf{0})$ is a time-like unit vector and we put $m = 1$. The functions D_{1-9} and D_{13-14} correspond to the denominators of the topology depicted in figure 2. The δ-functions in eq. (3.1) secure the energy conservation. Note that $n_{10-12} \leqslant 0$ and the prescription $-i0$ for D_{1-9} is implied.

Making the IBP reduction [16, 17] with `LiteRed` [23], we reveal 14 master integrals, see figure 3.

Note that the counter-term diagrams in figure 1 can also be expressed in terms of the four-loop master integrals in figure 1 although they have only three loops. To this end we multiply the corresponding integrals by $1 = \frac{-1}{\Gamma[1-d/2]} \int \frac{d^d l_2}{i\pi^{d/2} D_2}$. Then the contribution of counter-terms is expressed via the master integrals with unit mass tadpole loop, namely, via j_1 and j_5.

Since the integral family (3.1) contains no dimensionless free parameter, the differential equations method can not help directly. Therefore, there is a temptation to calculate the master integrals with the DRA (Dimensional Recurrence and Analyticity) method introduced in ref. [21]. This method is based on dimensional recurrence relations [20] and analytical properties of loop integrals as functions of space-time dimensionality d. Unfortunately, there is a nontrivial 2×2 diagonal block in the matrix of dimensional recurrence, corresponding to the integrals j_8 and j_9 which belong to one and the same sector.

JHEP12(2023)147

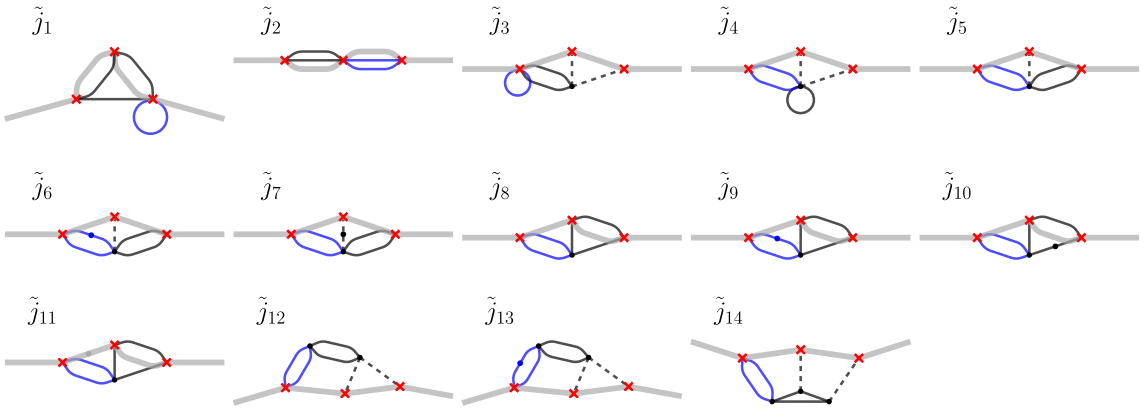

Figure 4. Master integrals of the two-scale family. Blue lines denote massive propagators with mass m.

Although it is, in principle, possible to apply the DRA method also for the cases with nontrivial diagonal 2×2 blocks as discussed in refs. [24, 25], its application in this case is much more laborious than that for the triangular matrix. Fortunately, for the present task we may apply a combined approach. First, we use the DRA method for all integrals but j_8, j_9, and j_{14} (the latter integral belongs to a super-sector of the sector of $j_{8,9}$). In order to obtain information about analytical properties necessary for fixing periodic functions in homogeneous parts of the solutions, we use the approach of ref. [26]. Namely, we choose the integrals which are obviously finite on a sufficiently wide vertical stripe in the complex plane of d. For example, in order to reveal the analytic properties of the most complicated integral j_{13} we use finiteness of the integral $j_{13f} =$ 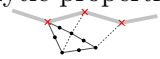 on the stripe $\operatorname{Re} d \in (3, 5]$. Reducing j_{13f} to the master integrals, we obtain a number of nontrivial constraints for the leading expansion terms of j_{13} on the basic stripe $(3, 5]$. The results of the DRA approach have the form of n-fold triangular sums with factorized summand and $n \leqslant 3$. We use `SummerTime` package [27] to calculate the ϵ-expansion of these sums with high precision and PSLQ algorithm [28] to recognize the result in terms of multiple zeta values.

Note that all three remaining integrals, j_8, j_9, and j_{14}, contain two disjoint massive loops. In order to calculate those integrals, we consider a family of integrals with different masses in these two loops. This family is defined by eqs. (3.1) and (3.2) where one should replace $D_1 \to \widetilde{D}_1 = m^2 - l_1^2$, $D_5 \to \widetilde{D}_5 = m^2 - (l_1 + q_1)^2$ and assume that $n_{6,7} \leqslant 0$ (in addition to $n_{10-12} \leqslant 0$). This family corresponds to the denominators of j_{14}, where the unit mass in the left-most fermion loop is replaced by m. Performing the IBP reduction, we reveal 14 master integrals depicted in figure 4. We obtain the differential system

$$\partial_m \tilde{j} = M(\epsilon, m)\tilde{j} \tag{3.3}$$

for the column $\tilde{j} = (\tilde{j}_1, \ldots, \tilde{j}_{14})^\intercal$ and reduce it to ϵ-form using `Libra` [29]. The general solution of eq. (3.3) is expressed in terms of harmonic polylogarithms [30]. The boundary conditions are put at $m \to 0$. We use expansion by regions [31, 32] to fix the required coefficients in the asymptotic expansion of integrals. The original integrals $j_{8,9,14}$ are recovered as

$$j_8 = \tilde{j}_8\Big|_{m=1}, \quad j_9 = \tilde{j}_9\Big|_{m=1}, \quad j_{14} = \tilde{j}_{14}\Big|_{m=1}. \tag{3.4}$$

JHEP12(2023)147

Note that other integrals in figure 3 which contain two disjoint fermion loops are also expressed in terms of the master integrals in figure 4:

$$j_1 = \tilde{j}_1\Big|_{m=1}, \quad j_3 = \tilde{j}_2\Big|_{m=1}, \quad j_4 = \tilde{j}_3\Big|_{m=1} = \tilde{j}_4\Big|_{m=1}, \quad j_7 = \tilde{j}_5\Big|_{m=1}, \quad j_{11} = \tilde{j}_{12}\Big|_{m=1}. \tag{3.5}$$

This provides a number of nontrivial cross checks of the obtained results for the master integrals.

Finally, we expand the diagrams in figure 1 in q and perform the Dirac algebra using `FeynCalc` [33]. After the IBP reduction and substitution of the results for the master integrals, we obtain our final result for the coefficient B in eq. (2.3). We present the contributions of diagrams in figures 1a and 1b separately:

$$B_{1a} = \frac{1456}{45}\mathrm{Li}_4\left(\tfrac{1}{2}\right) - \frac{4511\pi^4}{16200} + \frac{182\ln^4 2}{135} + \frac{274}{135}\pi^2\ln^2 2 - \frac{2387\pi^2\ln 2}{1080} + \frac{199\zeta_3}{45} + \frac{13057}{3240} + \frac{3703\pi^2}{5760} = 0.125181281880322\ldots, \tag{3.6}$$

$$B_{1b} = \frac{71\zeta_3}{56} - \frac{479}{756} + \frac{38401\pi^2}{217728} - \frac{283}{756}\pi^2\ln 2 = 0.070271202837585\ldots, \tag{3.7}$$

$$B = B_{1a} + B_{1b} = 0.195452484717907\ldots. \tag{3.8}$$

4 Conclusion

In the present paper we obtain the contributions of order $\alpha^2(Z\alpha)^6 m$ to the Lamb shift from radiative corrections to the Wichmann-Kroll potential depicted in figure 1. Numerically our result (3.8) appears to be rather small and compatible with the heuristic estimate $B = 0.13 \pm 0.13$ of refs. [14, 15]. For the calculation of master integrals we use a combination of the DRA method and the approach based on the differential equations. This calculation provides yet another example of the effectiveness of multiloop methods for obtaining analytic results in atomic physics.

Acknowledgments

The work has been supported by Russian Science Foundation under grant 20-12-00205.

References

[1] N. Bezginov et al., *A measurement of the atomic hydrogen Lamb shift and the proton charge radius*, *Science* **365** (2019) 1007 [INSPIRE].

[2] A. Grinin et al., *Two-photon frequency comb spectroscopy of atomic hydrogen*, *Science* **370** (2020) abc7776 [INSPIRE].

JHEP12(2023)147

[3] C.G. Parthey et al., *Precision Measurement of the Hydrogen-Deuterium 1S-2S Isotope Shift*, *Phys. Rev. Lett.* **104** (2010) 233001 [INSPIRE].

[4] A. Antognini et al., *Proton Structure from the Measurement of 2S-2P Transition Frequencies of Muonic Hydrogen*, *Science* **339** (2013) 417 [INSPIRE].

[5] CREMA collaboration, *Laser spectroscopy of muonic deuterium*, *Science* **353** (2016) 669 [INSPIRE].

[6] W. Xiong et al., *A small proton charge radius from an electron-proton scattering experiment*, *Nature* **575** (2019) 147 [INSPIRE].

[7] H.A. Bethe, *The electromagnetic shift of energy levels*, *Phys. Rev.* **72** (1947) 339 [INSPIRE].

[8] R. Karplus, A. Klein and J. Schwinger, *Electrodynamic Displacement of Atomic Energy Levels*, *Phys. Rev.* **84** (1951) 597 [INSPIRE].

[9] N.M. Kroll and F. Pollock, *Radiative Corrections to the Hyperfine Structure and the Fine Structure Constant*, *Phys. Rev.* **84** (1951) 594 [INSPIRE].

[10] R. Karplus and A. Klein, *Electrodynamic Displacement of Atomic Energy Levels. I. Hyperfine Structure*, *Phys. Rev.* **85** (1952) 972 [INSPIRE].

[11] M.I. Eides, H. Grotch and V.A. Shelyuto, *Theory of Light Hydrogenic Bound States*, Springer-Verlag, Berlin (2007) [DOI:10.1007/3-540-45270-2] [INSPIRE].

[12] V.A. Yerokhin, P. Indelicato and V.M. Shabaev, *Two-loop QED corrections with closed fermion loops*, *Phys. Rev. A* **77** (2008) 062510.

[13] V.A. Yerokhin, K. Pachucki and V. Patkós, *Theory of the Lamb Shift in Hydrogen and Light Hydrogen-Like Ions*, *Annalen Phys.* **531** (2019) 1800324 [arXiv:1809.00462] [INSPIRE].

[14] S.G. Karshenboim et al., *The Complete $\alpha^8 m$ Contributions to the 1s Lamb Shift in Hydrogen*, *Phys. Part. Nucl.* **53** (2022) 773 [INSPIRE].

[15] S.G. Karshenboim et al., *The Lamb shift of the 1s state in hydrogen: Two-loop and three-loop contributions*, *Phys. Lett. B* **795** (2019) 432 [arXiv:1906.11105] [INSPIRE].

[16] F.V. Tkachov, *A theorem on analytical calculability of 4-loop renormalization group functions*, *Phys. Lett. B* **100** (1981) 65 [INSPIRE].

[17] K.G. Chetyrkin and F.V. Tkachov, *Integration by parts: The algorithm to calculate β-functions in 4 loops*, *Nucl. Phys. B* **192** (1981) 159 [INSPIRE].

[18] A.V. Kotikov, *Differential equation method: The calculation of N point Feynman diagrams*, *Phys. Lett. B* **267** (1991) 123 [INSPIRE].

[19] E. Remiddi, *Differential equations for Feynman graph amplitudes*, *Nuovo Cim. A* **110** (1997) 1435 [hep-th/9711188] [INSPIRE].

[20] O.V. Tarasov, *Connection between Feynman integrals having different values of the space-time dimension*, *Phys. Rev. D* **54** (1996) 6479 [hep-th/9606018] [INSPIRE].

[21] R.N. Lee, *Space-time dimensionality D as complex variable: Calculating loop integrals using dimensional recurrence relation and analytical properties with respect to D*, *Nucl. Phys. B* **830** (2010) 474 [arXiv:0911.0252] [INSPIRE].

[22] P.A. Krachkov and R.N. Lee, *Two-loop corrections to Lamb shift and hyperfine splitting in hydrogen via multi-loop methods*, *JHEP* **07** (2023) 211 [arXiv:2306.13369] [INSPIRE].

JHEP12(2023)147

[23] R.N. Lee, *LiteRed 1.4: a powerful tool for reduction of multiloop integrals*, *J. Phys. Conf. Ser.* **523** (2014) 012059 [arXiv:1310.1145] [INSPIRE].

[24] R.N. Lee and K.T. Mingulov, *DREAM, a program for arbitrary-precision computation of dimensional recurrence relations solutions, and its applications*, arXiv:1712.05173 [INSPIRE].

[25] R.N. Lee and K.T. Mingulov, *Meromorphic solutions of recurrence relations and DRA method for multicomponent master integrals*, *JHEP* **04** (2018) 061 [arXiv:1712.05166] [INSPIRE].

[26] R.N. Lee and A.F. Pikelner, *Four-loop HQET propagators from the DRA method*, *JHEP* **02** (2023) 097 [arXiv:2211.03668] [INSPIRE].

[27] R.N. Lee and K.T. Mingulov, *Introducing SummerTime: a package for high-precision computation of sums appearing in DRA method*, *Comput. Phys. Commun.* **203** (2016) 255 [arXiv:1507.04256] [INSPIRE].

[28] H. Ferguson, D. Bailey and S. Arno, *Analysis of PSLQ, an integer relation finding algorithm*, *Math. Comput.* **68** (1999) 351.

[29] R.N. Lee, *Libra: A package for transformation of differential systems for multiloop integrals*, *Comput. Phys. Commun.* **267** (2021) 108058 [arXiv:2012.00279] [INSPIRE].

[30] E. Remiddi and J.A.M. Vermaseren, *Harmonic polylogarithms*, *Int. J. Mod. Phys. A* **15** (2000) 725 [hep-ph/9905237] [INSPIRE].

[31] M. Beneke and V.A. Smirnov, *Asymptotic expansion of Feynman integrals near threshold*, *Nucl. Phys. B* **522** (1998) 321 [hep-ph/9711391] [INSPIRE].

[32] A. Pak and A. Smirnov, *Geometric approach to asymptotic expansion of Feynman integrals*, *Eur. Phys. J. C* **71** (2011) 1626 [arXiv:1011.4863] [INSPIRE].

[33] V. Shtabovenko, R. Mertig and F. Orellana, *FeynCalc 9.3: New features and improvements*, *Comput. Phys. Commun.* **256** (2020) 107478 [arXiv:2001.04407] [INSPIRE].

JHEP12(2023)147